JBC RESEARCH ARTICLE

Anaplerosis by medium-chain fatty acids through complex interplay with glucose and glutamine metabolism

Received for publication, November 8, 2024, and in revised form, January 31, 2025 Published, Papers in Press, February 13, 2025,
https://doi.org/10.1016/j.jbc.2025.108307

Hannah M. German[1,2,*], **Jolita Ciapaite**[1,2], **Nanda M. Verhoeven-Duif**[1,2], **and Judith J. M. Jans**[1,2,*]

From the [1]*Section Metabolic Diagnostics, Department of Genetics, University Medical Centre Utrecht, Utrecht University, Utrecht;* [2]*United for Metabolic Diseases, the Netherlands*

Reviewed by members of the JBC Editorial Board. Edited by Qi-Qun Tang

The constant replenishment of tricarboxylic acid (TCA) cycle intermediates, or anaplerosis, is crucial to ensure optimal TCA cycle activity in times of high biosynthetic demand. In inborn metabolic diseases, anaplerosis is often affected, leading to impaired TCA cycle flux and ATP production. In these cases, anaplerotic compounds can be a therapy option. Triheptanoin, a triglyceride containing three heptanoate chains, is thought to be anaplerotic through production of propionyl- and acetyl-CoA. However, the precise mechanism underlying its anaplerotic action remains poorly understood. In this study, we performed a comprehensive *in vitro* analysis of heptanoate metabolism and compared it to that of octanoate, an even-chain fatty acid which only provides acetyl-CoA. Using stable isotope tracing, we demonstrate that both heptanoate and octanoate contribute carbon to the TCA cycle in HEK293 T cells, confirming direct anaplerosis. Furthermore, by using labeled glucose and glutamine, we show that heptanoate and octanoate decrease the contribution of glucose-derived carbon and increase the influx of glutamine-derived carbon into the TCA cycle. Our findings also point towards a change in redox homeostasis, indicated by an increased NAD^+/NADH ratio, accompanied by a decreased lactate/pyruvate ratio and increased *de novo* serine biosynthesis. Taken together, these results highlight the broad metabolic effects of heptanoate and octanoate supplementation, suggesting that therapeutic efficacy may strongly depend on specific disease pathophysiology. Furthermore, they underline the need for careful selection of fatty acid compound and concentration to optimize anaplerotic action.

The tricarboxylic acid (TCA) cycle is the major cellular amphibolic pathway located in the mitochondrial matrix. It captures energy from the oxidation of different nutrient molecules in the form of reducing equivalents, which subsequently fuel the production of ATP in oxidative phosphorylation (Fig. 1). Aside from its function in energy metabolism, the TCA cycle is also the main source of metabolic intermediates for several biosynthetic pathways such as gluconeogenesis (1), lipogenesis (2), and heme synthesis (3). As cells undergo active growth and proliferation, TCA cycle intermediates are shuttled into these branching pathways, a process referred to as cataplerosis (4).

To counteract the depletion of TCA cycle intermediates by cataplerosis, the TCA cycle is replenished through a process called anaplerosis. The most important anaplerotic enzyme is pyruvate carboxylase (PC; EC 6.4.1.1), which converts pyruvate to oxaloacetate (4, 5). Anaplerotic pathways play a central role in maintaining the pool of TCA cycle intermediates and ensuring its continuity, even in times of high energy consumption.

Several inborn metabolic diseases (IMDs) are characterized by impaired cellular energy metabolism due to the absence of a crucial enzyme in the catabolism of fatty acids, carbohydrates or amino acids. This results in diminished carbon entry and flux through the TCA cycle and ultimately decreased ATP production. Consequently, this leads to stimulation of the defective catabolic pathway, which is potentially damaging (6). In this context, anaplerotic compounds offer a potential for therapeutic intervention. The rationale behind this is that TCA cycle intermediates are replenished, not only providing energy for ATP production but also alleviating the breakdown of protein, sugars, and fats to increase ATP levels (6).

One such anaplerotic compound is triheptanoin, a synthetic medium-chain triglyceride (MCT) consisting of a glycerol backbone with three heptanoate (C7:0) chains attached. Mitochondrial β-oxidation of heptanoate yields two acetyl-CoA as well as one propionyl-CoA, which enters the TCA cycle as succinyl-CoA (Fig. 1). Triheptanoin has already been approved for use in long-chain fatty acid oxidation disorders (LC-FAODs) following numerous successful clinical trials (7–11) and is currently being tested for several other metabolic disorders (12–15). The current standard of care in several IMDs is medium-chain triglyceride (MCT) oil, which primarily consists of octanoate (C8:0). As octanoate is an even-chain fatty acid, its oxidation yields only acetyl-CoA. While this is an essential fuel for the TCA cycle, metabolism of acetyl-CoA does not result in a net increase in TCA cycle intermediates, as the introduced carbons are released as CO_2. In contrast, heptanoate oxidation produces acetyl-CoA and propionyl-CoA, which directly replenishes TCA cycle intermediates and has a different point of entry into the cycle. This suggests that heptanoate is a potentially more effective anaplerotic

* For correspondenceHannah M. German, H.M.German@umcutrecht.nl, Judith J. M. Jans, J.J.M.Jans@umcutrecht.nl.

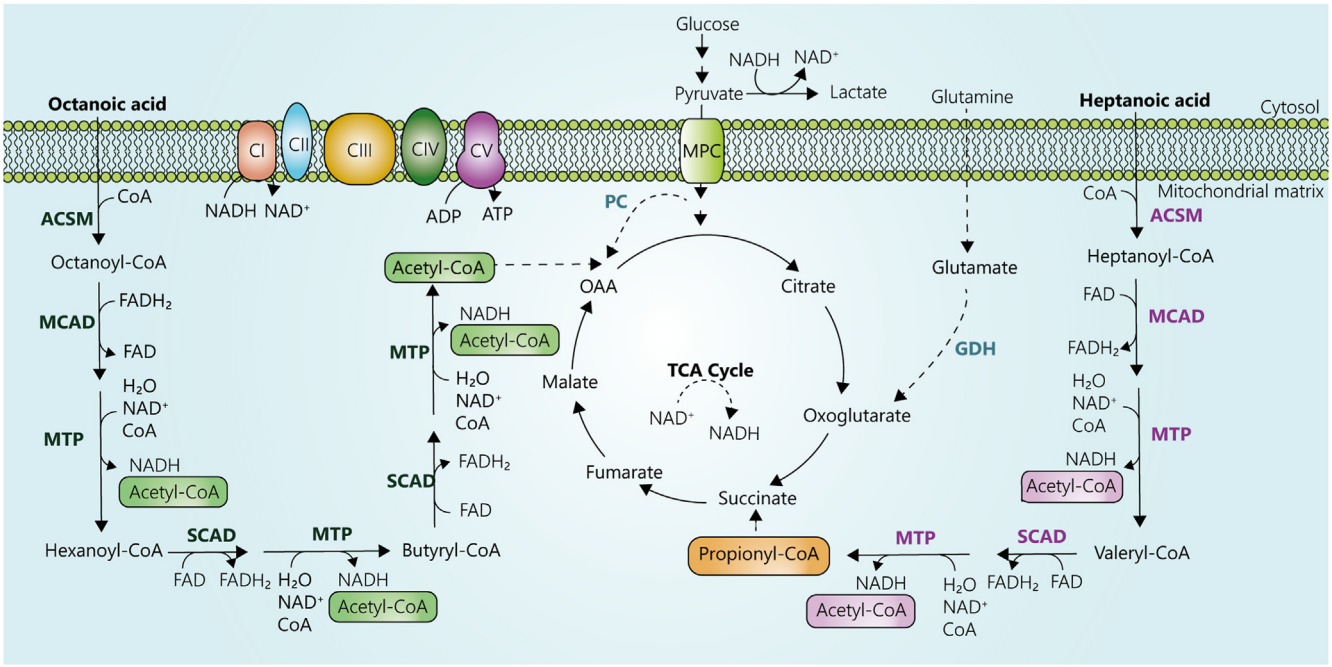

Figure 1. Metabolism of odd- and even-chain fatty acids. Schematic overview of metabolism of heptanoic acid (C7) and octanoic acid (C8) *via* beta-oxidation. Octanoic acid is oxidized to four molecules of acetyl-coA, which can combine with oxaloacetate to form citrate. Heptanoic acid yields two molecules of acetyl-coA and one molecule of propionyl-coA (C3), which can be converted to succinyl-coA and enter the TCA cycle as succinate. Both fatty acids also yield reducing equivalents in the form of NADH and $FADH_2$. ACSM, acyl-coA synthetase medium chain; CI-IV, complex I-IV; FATP, fatty acid transporter; GDH, glutamate dehydrogenase; GLUT, glucose transporter; MCAD, medium-chain acyl-CoA dehydrogenase; MPC, mitochondrial pyruvate carrier; MTP, mitochondrial trifunctional protein; OAA, oxaloacetate; SCAD, short-chain acyl-CoA dehydrogenase; SLC1A5, solute carrier family 1 member 5; α-KG, alpha-ketoglutarate.

treatment option. Despite extended application of triheptanoin in a clinical setting, in-depth mechanistic understanding of its anaplerotic action is still lacking. Expanding this knowledge may reveal the applicability of this compound for the treatment of a broader spectrum of IMDs that affect cellular energy metabolism.

Therefore, in the present study, we perform a comprehensive assessment of the *in vitro* metabolism of heptanoate and octanoate in HEK293 T cells, a cell model with well-characterized metabolic properties and a metabolic rate suitable for the observation of dynamic change over the experimental time course. Using stable isotope tracing, we investigated the extent to which these compounds directly contribute to the TCA cycle and assessed their interplay with other carbon sources. We show that both heptanoate and octanoate effectively contributed carbon to the TCA cycle, confirming anaplerosis. In addition, our data reveal a complex interaction among different carbon sources fueling the TCA cycle, indicating that a careful fine-tuning of fatty acid concentration is necessary for optimal anaplerotic action.

Results

Heptanoate and octanoate are metabolized through beta-oxidation in HEK293 T cells

The catabolism of triheptanoin is proposed to start in the intestine, where lipases release heptanoic acid from its glycerol backbone (16). Once released, heptanoic acid is passively transported into the mitochondria and enzymatically linked to CoA, thus forming the metabolically active heptanoyl-CoA (Fig. 1). Subsequently, heptanoyl-CoA is metabolized to one molecule of propionyl-CoA (C3) and two molecules of acetyl-CoA (C2) through a series of oxidation reactions, yielding two molecules of NADH and two molecules of $FADH_2$ in the process.

To investigate whether the uptake and metabolism of heptanoate takes place according to this proposed model *in vitro*, HEK293 T cells were supplemented with heptanoate and the formation of different acylcarnitines was assessed using direct-infusion high-resolution mass spectrometry (DI-HRMS). Acylcarnitines are formed during reversible shuttling of acyl units between free CoA and L-carnitine by acyltransferases. Therefore, they are representative of their corresponding CoA conjugates (17).

After 8 h of incubation, heptanoate-treated cells had significantly higher levels of C7-, C5- and C3-carnitines compared to untreated cells, indicating formation of heptanoyl-, valeryl- and propionyl-CoA (Fig. 2*A*). Furthermore, it was determined that supplementation of 3 mM heptanoate led to the most significant increases compared to lower concentrations (Fig. S1*A*). It was therefore decided to continue with this concentration in any further experiments. To rule out toxicity of the treatment, protein concentrations were used as a proxy for cell viability, in which we observed no significant differences between untreated and treated cells for either fatty acid (Fig. S1*B*). We therefore concluded that this concentration does not lead to toxicity within the experimental timeframe.

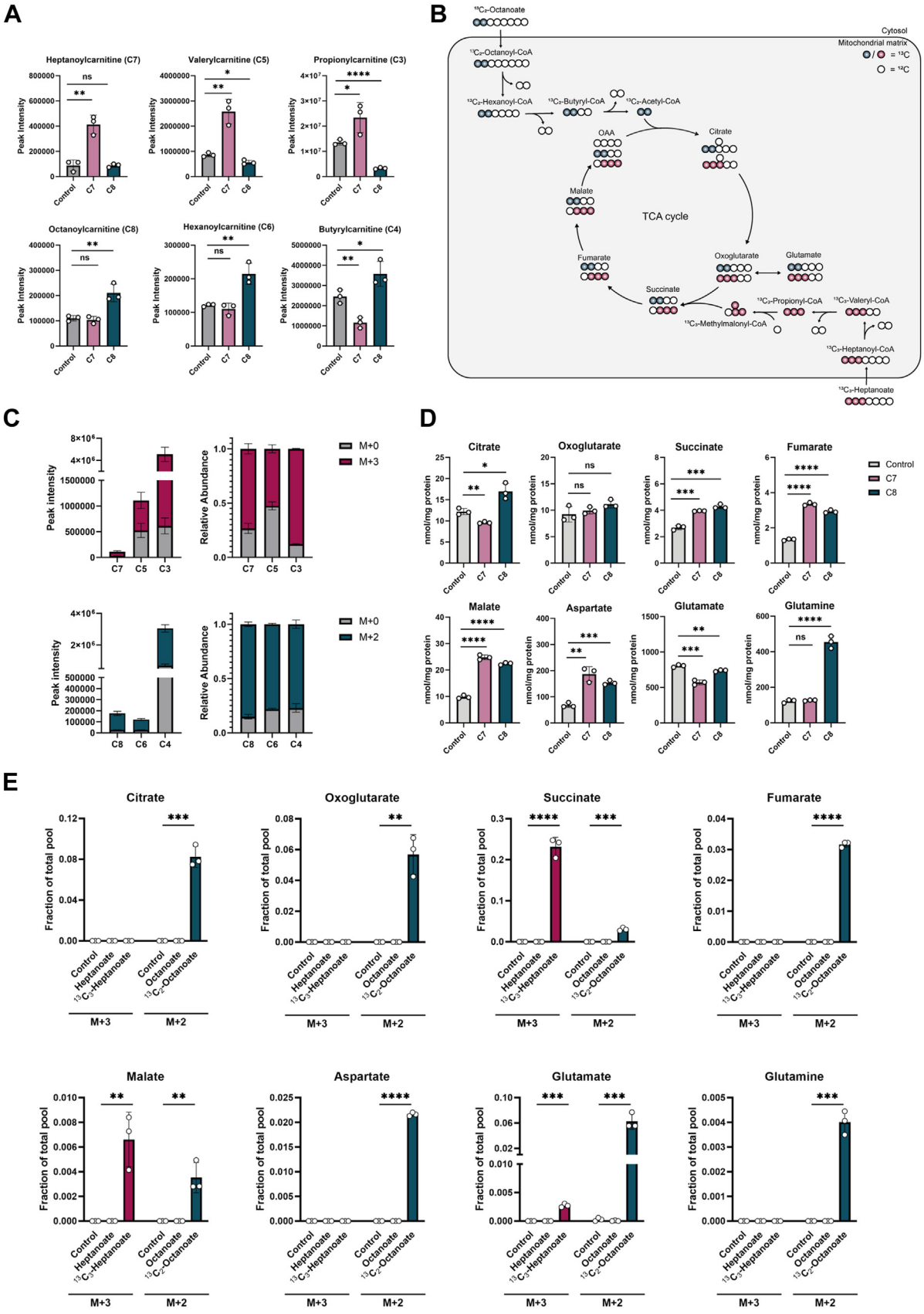

Figure 2. Heptanoic and octanoic acid are metabolized into the TCA cycle by HEK293 T cells. *A*, Peak intensities of C7-, C5-, C3-, C8-, C6- and C4-carnitines after 8h incubation with C7 (*pink*) or C8 (*blue*) compared to untreated controls (*grey*). Data are shown as mean ± SD of three technical replicates. *p*-values are indicated as $*p < 0.05$, $**p < 0.01$, $***p < 0.001$, and $****p < 0.0001$. Isobaric compounds are listed in Table S1. *B*, schematic overview of mitochondrial metabolism of $^{13}C_3$-heptanoate and $^{13}C_2$-octanoate. MDH2, malate dehydrogenase 2; TCA, tricarboxylic acid; OAA, oxaloacetate. *C*, summed

To confirm that the increased carnitine species are directly derived from the supplemented heptanoate and to exclude the contribution of isobaric compounds, cells were incubated with 5,6,7-$^{13}C_3$-heptanoic acid and the formation of corresponding $^{13}C_3$-acylcarnitines was assessed (Fig. 2, *B* and *C*). At 8 h, 73%, 53% and 88% of the C7- C5- and C3-carnitine pools respectively were comprised of the M + 3 isotopologue. This is indicative of metabolism of heptanoate through fatty acid oxidation.

An important component of current MCT treatment is octanoic acid (C8:0), a medium-chain fatty acid that, due to its even-length chain, does not result in the formation of anaplerotic propionyl-CoA. Rather, it is metabolized to hexanoyl-CoA (C6), butyryl-CoA (C4), and acetyl-CoA (C2; Fig. 1). As expected, octanoate treatment greatly increased levels of C8-, C6- and C4-carnitines compared to untreated or heptanoate-treated HEK293 T cells (Fig. 2*A*). Furthermore, no formation of odd-chain acylcarnitines was observed in octanoate-treated cells (Fig. 2*A*). When incubated with 7,8-$^{13}C_2$-octanoic acid, significant enrichment of M + 2 C8-, C6- and C4-carnitine was observed to 85%, 78%, and 77%, respectively (Fig. 2, *B* and *C*). Surprisingly, a significant decrease in acetylcarnitine was observed for both heptanoate and octanoate treatment, despite acetyl-CoA being a major by- and end-product of both heptanoate and octanoate oxidation (Fig. S2*A*). Treatment with $^{13}C_2$-octanoic acid did result in significant production of $^{13}C_2$-acetylcarnitine in HEK293 T cells, but it accounted only for 8% of the total acetylcarnitine pool (Fig. S2*B*). This indicates that under these culture conditions, mostly glucose-derived acetylcarnitine was formed.

To compare these observations to other cell types, A549 and fibroblast cells were treated with heptanoate and octanoate, and the levels of different acylcarnitines, as well as free carnitine, were measured and compared to those found in HEK293 T cells (Fig. S2*C*). As these cell models are less metabolically active, the incubation period was extended to 16 h. Similarly to HEK293 T cells, fibroblasts exhibited a significant increase in C5- and C3-carnitines upon heptanoate treatment, whereas octanoate mainly increased C4-carnitine levels (Fig. S2*C*). All cell types exhibited a decrease in free carnitine upon fatty acid treatment. Interestingly, no accumulation of the acylcarnitines species observed in HEK293 T cells and fibroblasts was observed in A549 cells.

Glycolysis-derived pyruvate is converted to acetyl-CoA by pyruvate dehydrogenase (PDH), after which it can enter the TCA cycle. It has been shown that fatty-acid-derived acetyl-CoA may inhibit PDH activity (18). Therefore, to further clarify the interplay between glucose- and fatty acid-derived carbons, we analyzed the effects of heptanoate and octanoate supplementation on TCA cycle intermediate concentrations and stable isotope labeling patterns.

First, the absolute concentrations of the TCA cycle intermediate as well as aspartate, glutamate, and glutamine were assessed after 8 h of incubation with heptanoate or octanoate (Fig. 2*D*). Octanoate, but not heptanoate treatment increased citrate levels, despite acetyl-CoA being a product of oxidation of both compounds. Theoretically, heptanoate oxidation results in less acetyl-CoA than octanoate oxidation, and thus may not lead to a significant accumulation of citrate. The other product, propionyl-CoA, enters the TCA cycle at a later step, which bypasses citrate synthesis. Succinate, fumarate, malate and aspartate levels were increased similarly by both treatments, despite their different points of entry. Glutamine accumulated in octanoate- but not heptanoate-treated HEK293 T cells, whereas glutamate was decreased in both conditions. 2-oxoglutarate levels remained unaffected.

To investigate to what extent these increases can be directly attributed to anaplerosis from fatty acids, UPLC-HRMS was used to assess the enrichment of ^{13}C-labeled TCA cycle intermediates after administration of $^{13}C_3$-heptanoate or $^{13}C_2$-octanoate. As shown before, $^{13}C_3$-heptanoate was metabolized to $^{13}C_3$-propionyl-CoA as well as two unlabeled acetyl-CoA molecules (Fig. 2*B*). $^{13}C_2$-Octanoate is metabolized to $^{13}C_2$-acetyl-CoA as well as three unlabeled acetyl-CoA, which can each be combined with oxaloacetate (OAA) to form citrate. In line with these different points of entry, $^{13}C_3$-propionyl-CoA exhibited the largest contribution to the succinate pool (~30%), whereas $^{13}C_2$-acetyl-CoA contributed mostly to the citrate pool (~10%; Fig. 2, *B* and *C*). $^{13}C_3$-labeling from propionyl-CoA was significantly enriched in malate but not fumarate, which might be due to low abundance of fumarate. $^{13}C_2$-labeling from acetyl-CoA was enriched in most other TCA cycle intermediates, as well as aspartate, glutamate and glutamine. These results confirm anaplerosis of heptanoate and octanoate *via* propionyl- and acetyl-CoA, respectively. Furthermore, they show metabolism of mainly acetyl-CoA-derived carbons into branching pathways compared to propionyl-CoA.

Despite the finding that heptanoate and octanoate directly contribute carbons to the TCA cycle, it is clear from our data that this contribution does not fully account for the significant total increase of TCA cycle intermediates, as the contribution is relatively small and does not directly correspond to the increase in total metabolite concentrations. As HEK293 T cells mostly use glucose and glutamine to fuel the TCA cycle, we hypothesized that fatty acid treatment may indirectly alter the fueling of the TCA cycle *via* these compounds. Therefore, we looked into the effect of heptanoate and octanoate treatment on glucose and glutamine metabolism.

Heptanoate and octanoate increase the availability of cytosolic NAD^+ while decreasing the entry of pyruvate into the TCA cycle

To investigate the effect on glucose metabolism, HEK293 T cells were incubated with $^{13}C_6$-glucose in combination with

absolute and relative intensities of M + 0 and M + 2/M + 3 acylcarnitines after incubation with $^{13}C_3$-heptanoate (*top panel*) or $^{13}C_2$-octanoate (*bottom panel*). Data are shown as mean ± SD of three technical replicates. *D*, absolute concentrations of TCA cycle intermediates in the presence or absence of C7/C8. Data are shown as mean ± SD of three technical replicates. *p*-values are indicated as $^*p < 0.05$, $^{**}p < 0.01$, $^{***}p < 0.001$, and $^{****}p < 0.0001$. *E*, Fractional M + 3/M + 2 labeling of TCA cycle intermediates after treatment with ($^{13}C_3$)-heptanoate (pink) or ($^{13}C_2$)-octanoate (*blue*) compared to untreated cells. Data are shown as mean ± SD of three technical replicates. *p*-values are indicated as $^*p < 0.05$, $^{**}p < 0.01$, $^{***}p < 0.001$, and $^{****}p < 0.0001$.

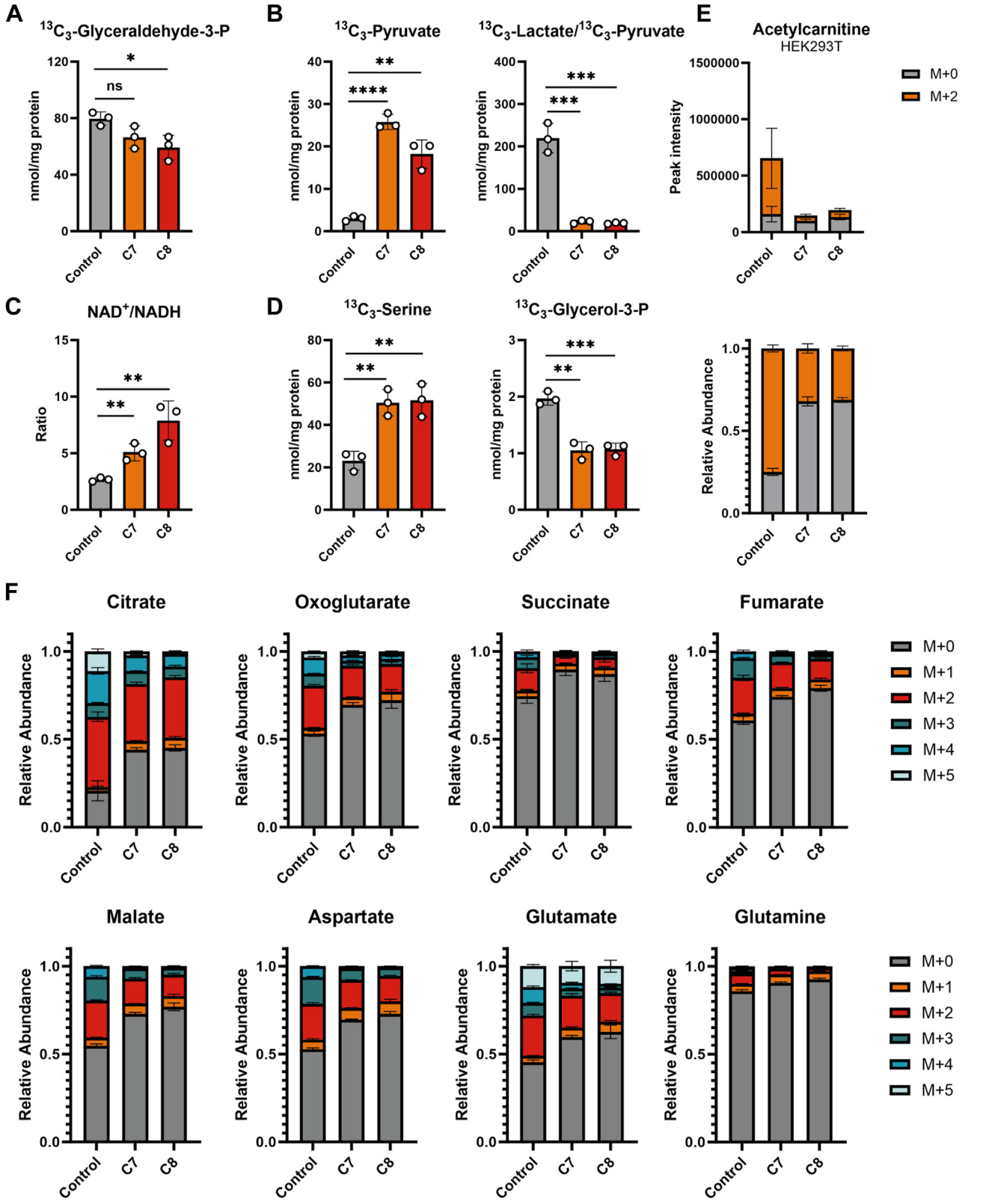

Figure 3. Glucose metabolism and redox homeostasis in fatty acid-treated HEK293 T cells. *A*, concentration of $^{13}C_3$-glyceraldehyde-3-phosphate, (*B*) Concentration of $^{13}C_3$-pyruvate and lactate/pyruvate ratio (*C*) NAD^+/NADH ratio, and (*D*) Concentrations of $^{13}C_3$ serine and $^{13}C_3$-glycerol-3-phosphate in presence or absence of C7 (*orange*) or C8 (*red*). Data are shown as mean ± SD of three technical replicates. *p*-values are indicated as $^*p < 0.05$, $^{**}p < 0.01$, $^{***}p < 0.001$, and $^{****}p < 0.0001$. *E*, Total and relative summed peak intensities of M + 0 and M + 2 acetylcarnitine in presence or absence of C7 or C8. Data are shown as mean ± SD of three technical replicates. *F*, relative isotopologue distribution of TCA cycle intermediates after incubation with $^{13}C_6$-glucose in presence or absence of C7 or C8. Data are shown as mean ± SD of three technical replicates. Isobaric compounds are listed in Table S1.

heptanoate or octanoate. The concentrations of ^{13}C-labeled glycolytic intermediates were subsequently measured with UPLC-HRMS. Cells treated with octanoate showed decreased levels of $^{13}C_3$-glyceraldehyde-3-phosphate, the substrate of glyceraldehyde-3-phosphate dehydrogenase (GAPDH; Fig. 3*A*). This is the only NAD^+-dependent and thus cellular redox-state sensitive enzyme of glycolysis. Furthermore, $^{13}C_3$-pyruvate levels were greatly increased in both conditions (Fig. 3*B*). This was not accompanied by an increase in intracellular $^{13}C_3$-lactate levels, resulting in a significantly decreased $^{13}C_3$-lactate/$^{13}C_3$-pyruvate ratio (Fig. S3*A*; Fig. 3*B*). Analysis of the medium showed increased levels of $^{13}C_3$-pyruvate but not -lactate, indicating that the excess pyruvate is mostly excreted (Fig. S3*B*).

As the intracellular lactate/pyruvate ratio is in equilibrium with the cytosolic NAD^+/NADH ratio, we assessed the absolute levels of NAD^+ and NADH and the ratio between these compounds (Fig. S3*C*; Fig. 3*C*). This showed an increased NAD^+/NADH ratio in fatty acid-treated cells, mainly due to an increase in NAD^+ levels. This increased ratio may be limiting the production of lactate by lactate dehydrogenase.

Aside from the decreased lactate/pyruvate ratio, several other indicators were found pointing towards higher availability of cytosolic NAD^+. The first enzyme of *de novo* serine biosynthesis, phosphoglycerate dehydrogenase (PHGDH), is NAD^+-dependent. Glycerol-3-phosphate dehydrogenase, on the other hand, regenerates NAD^+ as part of the glycerol-phosphate shuttle. Accordingly, previous studies have shown that depletion of cytosolic NAD^+ aberrates serine biosynthesis and causes the accumulation of glycerol-3-phosphate (G3P) as a compensatory mechanism (19). In heptanoate- and octanoate-treated cells, levels of $^{13}C_3$-serine were increased, whereas levels of $^{13}C_3$-G3P were decreased (Fig. 3*D*). Both of these observations, together with the decreased lactate/pyruvate ratio and increased total NAD^+/NADH ratio, are indicative of a higher availability of NAD^+ in the cytosol following fatty acid treatment. A higher NAD^+/NADH ratio supports oxidative metabolism and thus promotes ATP production. This could therefore be of interest for treatment of IMDs in which energy metabolism is impaired.

To further investigate the modulation of glucose metabolism by fatty acids, we used DI-HRMS on $^{13}C_6$-glucose-treated cells. In non-cancerous oxygenated cells, the main fate of pyruvate is conversion to acetyl-CoA and subsequent entry into the TCA cycle. When $^{13}C_3$-pyruvate is formed from $^{13}C_6$-glucose, it is metabolized to $^{13}C_2$-acetyl-CoA and $^{13}C_2$-citrate. In untreated HEK293 T cells, $^{13}C_2$-acetylcarnitine comprised ca. 75% of the total pool following 8 h of incubation with $^{13}C_6$-glucose (Fig. 3*E*). This indeed indicates that under normal conditions, glycolysis-derived pyruvate is the main source for acetyl-CoA. Cells treated with medium-chain fatty acids, however, showed greatly decreased relative and absolute levels of $^{13}C_2$-acetylcarnitine, pointing towards decreased contribution of glucose-derived acetyl-CoA to the total acetyl-CoA pool. This is consistent with the observed accumulation and excretion of glucose-derived pyruvate and decreased total acetylcarnitine levels.

In A549 cells, the baseline contribution of glucose to the acetyl-CoA pool is smaller (ca. 40%) as these cells have a larger flux from pyruvate to lactate (Fig. S3*D*). Despite this, a similar decrease in $^{13}C_2$-acetylcarnitine was observed following fatty acid treatment as in HEK293 T cells. In both cell types, total acetylcarnitine pools decreased, but the unlabeled pools did not change significantly in any of the conditions. Therefore, our data unambiguously show that in both cell types, the decrease in acetylcarnitine levels in response to heptanoate and octanoate treatment is the result of decreased pyruvate entry into the TCA cycle.

Both heptanoate and octanoate increased the unlabeled fraction of several TCA cycle intermediates in HEK293 T cells, most notably malate, fumarate, and aspartate (Figs. 3*F*; S3*E*). Concurrently, the fraction that is labeled by glucose decreases, indicating that treatment with fatty acids inhibits the influx of glucose-derived carbons into the TCA cycle. This is consistent with the previous finding that glucose-derived pyruvate accumulates upon fatty acid treatment, whereas acetylcarnitine levels are decreased. This is likely the consequence of increased fatty acid anaplerosis, decreasing the need for glucose-derived carbons to fuel the TCA cycle. As mentioned earlier, this may result in inhibition of PDH, which is a known effect of increased levels of fatty-acid derived acetyl-CoA.

Heptanoate and octanoate alter catabolism of glutamine into aspartate

Glutamine is the major source of TCA cycle intermediates in HEK293 T cells and is thus rapidly taken up and metabolized. To look at the initial effects of fatty acid treatment on TCA cycle metabolism, we incubated HEK293 T cells with $^{13}C_5$-glutamine as well as heptanoate or octanoate for 3 h and assessed the levels and isotopologue distributions of TCA cycle intermediates. The analysis of steady state labeling patterns showed that all pools of TCA cycle intermediates were almost completely $^{13}C_5$-glutamine-derived (Fig. 4*A*). Due to the shorter incubation time, the accumulation of TCA cycle intermediates observed in previous experiments was not observed here, with the exception of aspartate (Fig. S4*A*). The fractional labeling pattern of aspartate also showed an increase in the M + 4 isotopologue fraction. In addition to the accumulation of aspartate, heptanoate and octanoate were found to both significantly decrease the fractional turnover of glutamine-derived oxidative TCA cycle intermediates (Figs. 4*B*; S4*B*). The strong accumulation of aspartate may be the result of the increased cytosolic NAD^+/NADH ratio, limiting the NADH-dependent activity of malate dehydrogenase 1, or of the decreased levels of acetyl-CoA which may cause OAA accumulation. This accumulation consequently results in decrease in fractional turnover of TCA cycle intermediates upstream of aspartate and may explain the total increases found in the levels of these intermediates in previous experiments. Accordingly, when HEK293 T cells are incubated in the absence of glutamine, the increase of TCA cycle intermediates by heptanoate and octanoate is almost completely abolished (Fig. S4*C*). This indicates that the increase in TCA cycle intermediates after medium-chain fatty acid treatment is largely dependent on glutamine metabolism.

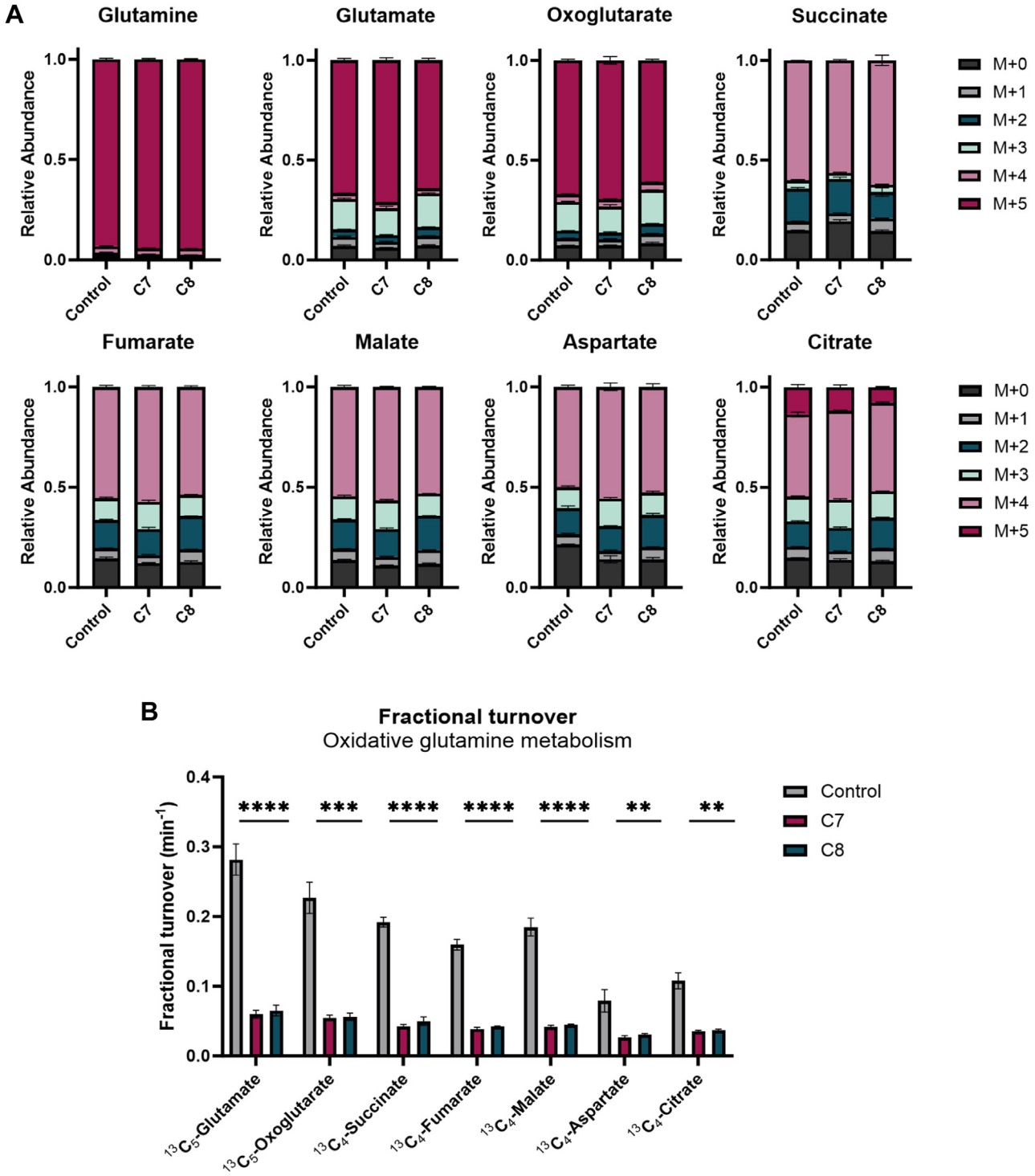

Figure 4. Glutamine metabolism in fatty acid-treated HEK293 T cells. *A*, summed relative isotopologue concentrations of TCA cycle intermediates after incubation with $^{13}C_5$-glutamine in the presence or absence of C7 or C8. Data are shown as mean ± SD of three technical replicates from two independent experiments. *B*, fractional turnover (K) of oxidative TCA cycle metabolites derived from $^{13}C_5$-glutamine in the presence or absence of C7 or C8. Data are shown as mean ± SD of three technical replicates averaged from two independent experiments. Parametric unpaired t-tests were followed by Benjamini-Hochberg's procedure for multiple testing. Adjusted *p*-values are indicated as $^*p < 0.05$, $^{**}p < 0.01$, $^{***}p < 0.001$, and $^{****}p < 0.0001$.

Taken together, our data show a complex interplay between different carbon sources to fuel the TCA cycle (Fig. 5). While direct TCA cycle anaplerosis by medium-chain fatty acids plays a role to some extent, it becomes clear that indirect effects through other carbon sources as well as modulation of redox homeostasis significantly influence their anaplerotic action. This highlights the need for a specific fine-tuning of different nutrient concentrations to optimize the potential of anaplerotic therapies in patients.

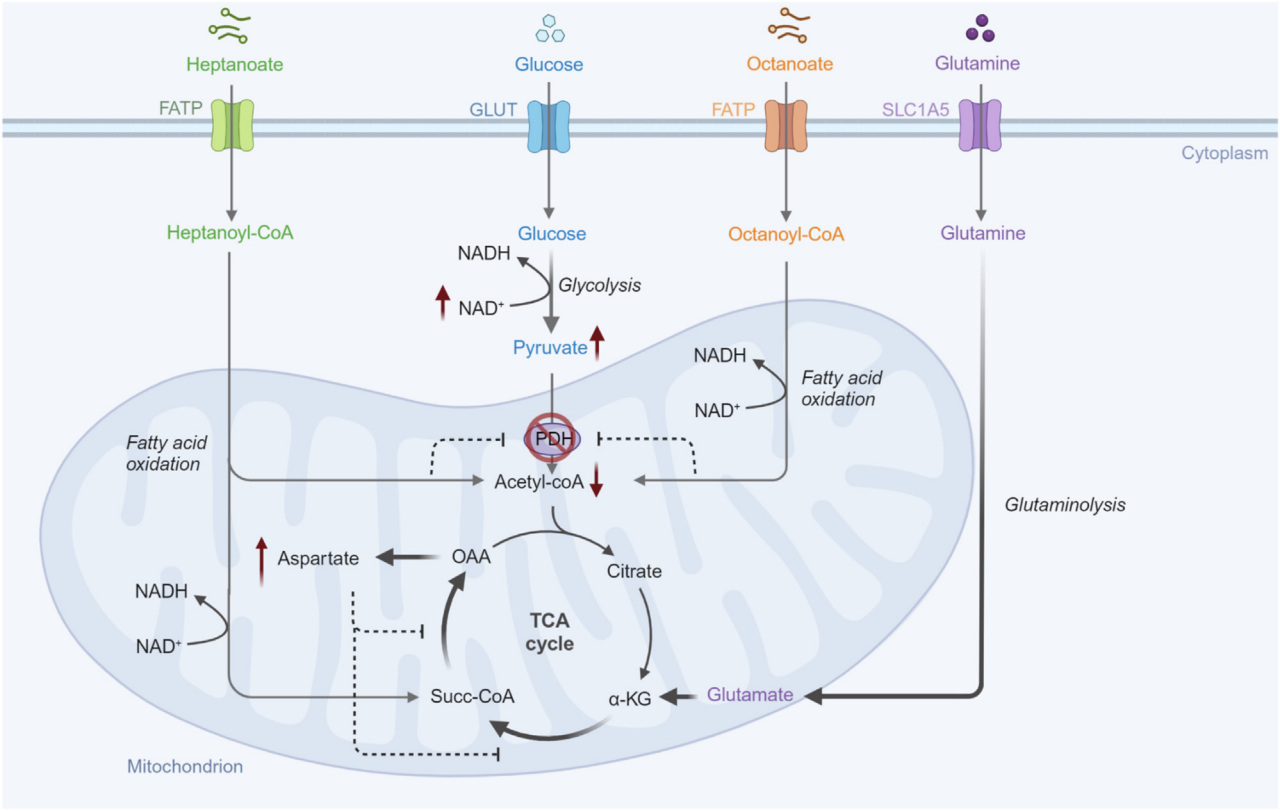

Figure 5. Overview of metabolic interplay between medium-chain fatty acids, glucose and glutamine in HEK293 T cells. Heptanoate and octanoate are both taken up and oxidized through fatty acid oxidation. Heptanoate yields acetyl- and propionyl-CoA, whereas octanoate yields only acetyl-CoA. This presumably has an inhibitory effect on pyruvate dehydrogenase, leading to the accumulation of glycolysis-derived pyruvate and decreased acetyl-CoA. Medium-chain fatty acids increase levels of NAD+, leading to increased serine production and decreased glycerol-3-phosphate. Lastly, both heptanoate and octanoate cause increased flux from glutamine into aspartate, leading to the accumulation of aspartate and consequent upstream increases in TCA cycle intermediate levels. a-KG, alpha-ketoglutarate; FATP, fatty acid transporter; GLUT, glucose transporter; OAA, oxaloacetate; PDH, pyruvate dehydrogenase; SLC1A5, solute carrier family 1 member 5; succ-CoA, succinyl-CoA; TCA, tricarboxylic acid. Adapted from: "Overview of BCAA Catabolic Enzymes" by BioRender.com (2023). Retrieved from https://app.biorender.com/biorender-templates (accessed on October 22, 2024).

Discussion

Medium-chain fatty acids have been implicated as potential therapeutics in several metabolic disorders, for their ability to replenish the TCA cycle with intermediates and their ability to increase ATP production. Although it has been hypothesized that decreased TCA cycle flux underlies many disease pathologies, it is often not possible to demonstrate this *in vivo* due to the low abundance of oxaloacetate, the acceptor of acetyl-CoA (20). Furthermore, due to the limited knowledge of the extent to which medium-chain fatty acids are anaplerotic, it remains difficult to predict whether they will be beneficial to a patient.

While current anaplerotic therapies are mainly based on even-chain fatty acids, the view has been shifting in recent years favoring odd-chain fatty acids. Even-chain fatty acids can only provide acetyl-CoA to the TCA cycle, whereas odd-chain fatty acids can provide both acetyl- and propionyl-CoA, making them potentially more effective. However, strong evidence for this on a metabolic level is still lacking. Consequently, one can only determine the efficacy of medium-chain fatty acid therapy *a posteriori* by assessing the alleviation of symptoms (20). This further highlights the need for a solid mechanistic basis on which the decision for anaplerotic therapy can be made.

To address this knowledge gap, we investigated the *in vitro* uptake and metabolism of heptanoic acid, the free fatty acid form of triheptanoin, and octanoic acid, a major component of MCT treatment. We demonstrate that both compounds are taken up and metabolized by HEK293 T cells and that this leads to increased levels of several TCA cycle intermediates, mainly malate, fumarate, and aspartate. Our data suggests that this is partially achieved by the direct contribution of carbons to the TCA cycle, confirming anaplerosis but more so by increased flux from glutamine into aspartate *via* the TCA cycle. This is most likely linked to the observed increase of the NAD^+/NADH ratio, limiting the activity of the cytosolic half of the malate-aspartate shuttle. On the other hand, catabolism of glucose into the TCA cycle was found to be decreased by fatty acid supplementation, leading to accumulation of pyruvate and decreased levels of acetyl-CoA. This is in line with previous studies showing that increased fatty acid oxidation limits the activity of pyruvate dehydrogenase (18). Decreased levels of acetyl-CoA may limit the production of citrate, leading to increased production of aspartate from OAA. Surprisingly, whereas propionyl-CoA was found to contribute significantly more carbon to succinate and acetyl-CoA to citrate, both compounds elicited similar changes in total metabolite pools. Other factors such as the lactate/pyruvate and NAD^+/NADH

ratios were also increased similarly by both compounds, suggesting a similar effect on intracellular redox homeostasis. This together indicates that in this model, the synergistic effects of heptanoate-derived propionyl- and acetyl-CoA do not show a significantly higher effect on TCA cycle intermediate levels or redox homeostasis compared to octanoate-derived acetyl-CoA.

This is surprising, as it has been hypothesized that heptanoate has a greater anaplerotic effect than octanoate due to its additional point of entry into the TCA cycle. The lack of significant differences observed may be attributed to the specific experimental conditions used in this study, such as the timeframe, nutrient availability, and specific cell models. Under these conditions, propionyl-CoA might not be sufficiently used as a source of TCA cycle intermediates. Additionally, despite the use of reduced glucose concentrations to mitigate the effects of glucose-derived acetyl-CoA, glycolysis could still restrict fatty acid oxidation in this model. This could decrease the influx of fatty acid-derived substrates to the TCA cycle. Lastly, *in vitro* cell models, like the ones used in this study, do not fully replicate tissue-specific metabolic mechanisms, in which the differences between these fatty acids might be more pronounced. Therefore, future studies in more physiologically and clinically relevant systems, such as *in vivo* models or other cell types, may help to further elucidate potential differences between heptanoate and octanoate anaplerosis. Such models also enable the assessment of other parameters, such as side effects and accurate dosing.

We found that fatty acid supplementation significantly increased the NAD^+/NADH ratio, which supports oxidative metabolism and mitochondrial function, potentially leading to increased ATP production. Furthermore, as shown by our results, an increased NAD^+/NADH ratio promotes NAD^+ -dependent pathways such as *de novo* serine biosynthesis. This is relevant in the context of IMDs where a decreased NAD^+/NADH ratio is observed due to an enzymatic defect affecting the TCA cycle, oxidative phosphorylation, or fatty acid oxidation. Therefore, the increased ratio observed in this study could have therapeutic benefits in such diseases. However, this effect would likely depend on the specific defect and tissue type.

These results are in line with several previous comparative studies on the effects of odd- and even-chain fatty acids. It was found in swine models that odd- and even-chain fatty acids elicited an equal increase in propionyl-CoA flux relative to acetyl-CoA (21). This goes against the notion that only odd-chain fatty acids are anaplerotic through succinyl-CoA, and that thus odd-chain fatty acids are more efficient at maintaining high levels of TCA cycle intermediates or rescuing a disturbed redox balance. Similarly, it was found in very long chain acyl-CoA dehydrogenase (VLCAD)-deficient fibroblasts that both heptanoate and octanoate protect against glutathione depletion induced by metabolic stress in an equal manner (22).

In a clinical trial conducted by Gillingham *et al.* (10), in which patients with LC-FAOD received triheptanoin or trioctanoin treatment for a duration of 4 months, it was found that heptanoate treatment significantly improved cardiorespiratory fitness compared to octanoate treatment. This suggests that C7 may be more beneficial for patients suffering with cardiomyopathy. It has also been reported that patients with LC-FAOD receiving triheptanoin experienced less major clinical events compared to patients receiving even-chain MCT or no treatment (23).

Okere *et al.* (24) found that heptanoate increased malate and fumarate levels, whereas hexanoate increased only succinate levels. The fact that even-chain fatty acids increase succinate is a surprising finding, as presumably, only odd-chain fatty acids can provide anaplerosis through succinyl-CoA. However, our results suggest this could also be the result of increased glutamine anaplerosis. It was found in the same study that despite an increase in TCA cycle intermediates, heptanoate did not increase the contractile function of the heart. This highlights that a change in TCA cycle intermediate levels does not always signify a change in energy metabolism and underlines the importance of further elucidating the effects of medium-chain fatty acids on energy metabolism.

Our study found that fatty acid supplementation stimulates the production of aspartate from glutamine, making it a potentially interesting therapeutic option for patients with low aspartate levels. Furthermore, glutamine is an important anaplerotic substrate when biosynthetic demand is high or under conditions of metabolic stress. This is illustrated by the fact that in many cancer cells, a shift occurs towards higher glutamine consumption to fuel the TCA cycle and support biosynthesis. In the context of IMDs, where mitochondrial dysfunction or defects in energy metabolism lead to disrupted TCA cycle activity, the ability to increase glutamine flux could help to restore TCA cycle function. Therefore, manipulating the catabolism of glutamine in combination with the use of fatty acids as anaplerotic substrates may be promising as a treatment strategy for inborn metabolic diseases. Studies in rat enterocytes however showed that octanoate supplementation eventually decreased glutamine utilization, which suggests that it can replace glutamine as a source of TCA cycle intermediates over longer periods of supplementation (25). This implies that prolonged periods of fatty acid supplementation may be necessary for certain effects to take place. For instance, it was found that long-term treatment with medium-chain fatty acids results in disturbance of the hepatic and cardiac fatty acid composition, and even-chain fatty acids specifically caused massive upregulation of peroxisomal β-oxidation in WT and VLCAD-deficient mice (26). Along with the observation that long-term exposure to medium-chain fatty acids causes dramatic accumulation of visceral fat and serum-free fatty acids in these mice, this suggests that medium-chain fatty acids, while partly being catabolized to provide energy, are also elongated and stored as long-chain fatty acids, which may cause metabolic syndrome-like symptoms. Additionally, it has been reported that VLCAD-deficient mice on a long-term MCT diet developed severe hepatic steatosis (27). Although none of these symptoms have been observed in humans thus far, this does highlight the importance of longer-term follow-up studies in patients to assess the safety and occurrence of adverse effects (28). Additionally, this underlines the difference in metabolic effects between different tissues and cell types,

which was also observed in this study. While our study provides a comprehensive understanding of the anaplerotic potential of heptanoate and octanoate, we acknowledge that it has several limitations. Future work is needed to validate our findings *in vivo*, which would offer relevant insights into the physiological relevance of these fatty acids and their therapeutic potential. This would also allow for an assessment of potential side effects and appropriate treatment dosing and duration. Additionally, it is of interest to study the effects of medium-chain fatty acids in different cell models and tissues, as metabolic effects may vary between these different cell types.

In conclusion, we demonstrated that *in vitro*, heptanoate and octanoate are metabolized *via* β-oxidation into the TCA cycle. While octanoate is mostly anaplerotic *via* citrate and heptanoate *via* succinate, they contribute equally to levels of most TCA cycle intermediates and to the increase of the cytosolic NAD^+/NADH ratio. We showed that fatty acid supplementation largely blocked the entry of glucose-derived pyruvate into the citric acid cycle, leading to decreased levels of acetyl-CoA. Lastly, we showed that the increased levels of TCA cycle intermediates can largely be attributed to an increase in glutamine anaplerosis in the direction of aspartate, ultimately leading to decreased turnover of glutamine-derived oxidative TCA cycle intermediates. These findings provide novel insights into the metabolic effects of odd- and even-length medium-chain fatty acids and suggest that these compounds can potentially be beneficial for a wide range of metabolic diseases in which TCA cycle flux is decreased. Our results indicate their effect on redox homeostasis is very similar, but when it comes to TCA cycle anaplerosis their efficacy might depend on the specific disease pathophysiology. Acetyl-CoA-derived carbon could be traced back in all TCA cycle intermediates as well as branching pathways, indicating it may be useful for general replenishment of the TCA cycle and to increase flux to glutamate and aspartate. Propionyl-CoA-derived carbon contributes mostly to the succinate and malate pool, indicating it may be useful in disorders leading to depletion of this arm of the TCA cycle. To further investigate this, it would be of interest to study the effect of heptanoate and octanoate under metabolic stress conditions, such as *in vitro* models mimicking inborn metabolic disorders. This would provide a physiologically relevant environment to study their efficacy and allow for a deeper understanding of their therapeutic potential. Additionally, the concentration of fatty acids used relative to glucose and protein intake may be an important factor, as this may have significant effects on glucose and glutamine catabolism.

Experimental procedures

Cell culture

HEK293 T cells and human skin fibroblasts were cultured in Dulbecco's Modified Eagle Medium (DMEM), high glucose, GlutaMAX, pyruvate (Thermo Fisher Scientific) supplemented with 10% v/v heat-inactivated fetal bovine serum (FBS; Thermo Fisher Scientific, #10270106) and 1% v/v penicillin/streptomycin (P/S; Thermo Fisher Scientific, #15140122). A549 cells were cultured in Roswell Park Memorial Institute (RPMI) 1640 (Thermo Fisher Scientific, #21870076) supplemented with 2 mM L-glutamine (Sigma-Aldrich), 10% v/v heat-inactivated FBS, and 1% v/v P/S. Cells were maintained at 37 °C and 5% CO_2 in a humidified incubator and passaged upon reaching confluence. Media were changed every 48h.

Collection of cell lysates for metabolite extraction

HEK293 T, A549, and fibroblast cell lines were plated in triplicate in 6-well culture plates (Corning) and grown until ca. 80% confluency. Medium was replaced 16 h before harvesting by glucose- and serum-free medium containing 0 or 3 mM heptanoic or octanoic acid (Sigma-Aldrich) and 5 mM D-Glucose (Sigma-Aldrich) to mimic physiological glucose concentrations. Cells were harvested by washing cells once (HEK293 T) or twice (A549 and fibroblasts) with 1.5 ml phosphate-buffered saline (PBS), followed by scraping twice with 350 µl ice-cold methanol absolute. Methanol cell extracts were transferred into 1.5 ml Eppendorf tubes and centrifuged at 16,200 x g for 10 min at 4 °C. Supernatants were transferred to fresh Eppendorf tubes and stored at −80 °C until further analysis.

Isotope tracing experiments

For isotope tracing experiments, HEK293 T cells were plated as described above. The medium was replaced 16 h before the start of the experiment with a serum-free medium containing 0 or 3 mM heptanoic or octanoic acid. The next day, medium was replaced with serum-free medium containing 0 or 3 mM heptanoic or octanoic acid and the isotope-labeled substrate (5 mM $^{13}C_6$-glucose or 4 mM $^{13}C_5$-glutamine (Cambridge Isotope Laboratories, Inc.)). For labeled fatty acid isotope tracing, medium was replaced with serum-free medium containing 3 mM $^{13}C_2$-octanoic acid or $^{13}C_3$-heptanoic acid (Sigma-Aldrich) or 3 mM unlabeled octanoic or heptanoic acid. At the indicated time points, cells were harvested as described earlier. Incubation times were selected to allow sufficient incorporation of labeled substrates into downstream metabolites to reach isotopic steady state. $^{13}C_5$-Glutamine, $^{13}C_3$-heptanoate and $^{13}C_2$-octanoate tracing experiments were performed in the presence of 5 mM D-Glucose to mimic physiological concentrations.

Direct infusion high-resolution mass spectrometry analysis

Methanol cell extracts were diluted to the lowest protein concentration as determined by a Pierce BCA protein assay. 70 µl methanol cell extract was combined with 70 µl internal standard solution and 60 µl 0.3% formic acid as described by Haijes *et al*. (29). Samples were filtered through a methanol pre-conditioned 96-well filter plate (Pall Corporation) with a vacuum manifold. The filtrate was collected in a 96-well PCR plate (Thermo Fisher Scientific).

Samples were analyzed by direct infusion high-resolution mass spectrometry (DI-HRMS) using a TriVersa Nanomate system (Advion) with Chipsoft software (version 8.3.3, Advion)

coupled to a Q Exactive Plus hybrid quadrupole-Orbitrap mass spectrometer (Thermo Fisher Scientific). 13 µl sample followed by a 2 µl air gap was aspirated into a pipette tip and delivered through an electrospray ionization (ESI) chip at a nitrogen gas pressure of 0.5 PSI and a spray voltage of 1.6 kV. Other parameters included a mass range of 70 to 600 m/z, run time of 3 min (1.5 min positive mode, 1.5 min negative mode), resolution of 140.000, AGC target 3 x 10^6, maximum injection time 200 ms, capillary temperature 275 °C, s-Lens RF factor of 70 and sample tray was cooled at 18 °C. Mass calibration was performed prior to each measurement sequence. All samples were measured in duplicate.

Data acquisition was performed with XCalibur software (Version 3.0, Thermo Fisher Scientific). Peak annotation was performed using an in-house peak calling pipeline in R (Source code available at: https://github.com/UMCUGenetics/DIMS). Mass peaks were annotated using the Human Metabolome Database (HMDB; version 3.6) within a range of 5 parts per million (Table S1). Annotation of isotope-labeled metabolites was done as described in Meijer *et al.* (30). For each sample, the mean intensity of the duplicate injections was reported for each mass peak.

LC-MS analysis of TCA cycle intermediates

UPLC-HRMS analysis of TCA cycle intermediates was performed as described before (30). Calibration standards were prepared in a range from 0.15 to 80 µM. The internal standard mix consisted of $^2H_3$-lactate, $^2H_3$-malate, $^2H_4$-citrate, $^2H_4$-succinate, $^2H_4$-fumarate, $^2H_5$-glutamine, $^2H_3$-glutamate and $^2H_4$-α-ketoglutarate (Sigma-Aldrich; 100 µM). 20 µl internal standard mix was added to 400 µl methanol cell extract or 50 µl calibration standard. Samples were evaporated under a gentle nitrogen flow at 40 °C. Dry extracts were reconstituted in 25 µl 0.1% NaOH and 25 µl 10 mg/ml O-(2,3,4,5,6-pentafluorobenzyl)hydroxylamine (PFBHA) in Milli-Q water. Samples were derivatized in a thermomixer for 30 min at 1000 rpm and transferred to LC vials.

Samples were analyzed on an Ultimate 3000 UHPLC system (Thermo Fisher Scientific) coupled to a Q Exactive HF hybrid quadrupole-Orbitrap mass spectrometer (Thermo Fisher Scientific) equipped with an electrospray ionization (ESI) source. The equipment was routinely purged and recalibrated before each measurement sequence. 5 µl sample was injected on a Sunshell RP-Aqua column (3 x 150 mm, 2.6 um; ChromaNik Technologies Inc., Osaka, Japan) with a flow rate of 0.6 ml/min, column oven temperature of 40 °C and autosampler temperature of 10 °C. Solvent A was comprised of 0.1% formic acid (v/v) in Milli-Q water and solvent B was comprised of 0.1% formic acid (v/v) in acetonitrile. Gradient elution was as follows: 0 to 2.75 min isocratic 0% B, 2.75 to 3.5 min linear gradient from 0 to 70% B 3.5 to 6.5 min isocratic 70% B, 6.5 to 6.7 min linear gradient from 70-0% B, 6.7 to 10 min column equilibration at 0% B. The mass spectrometer was operated in negative ionization mode with the following scan parameters: mass range of 70 to 400 m/z; capillary voltage of 4 kV, AGC target of 1 x 10^6, resolution of 240,000, maximum injection time of 200 ms, capillary temperature of 300 °C and an S-lens RF level of 65. Data acquisition was done using Xcalibur software. To identify and reduce potential contamination, blanks were measured between samples. Peak integration was done using Tracefinder software (Thermo Fisher Scientific; version 4.1). For representative chromatograms of endogenous metabolites and internal standards, see Fig. S5*A–B*.

LC-MS analysis of glycolysis intermediates and NAD(H)

UPLC-HRMS analysis of glycolysis intermediates and NAD(H) was performed as described previously (31). Calibration standards were prepared in a range from 0.1 to 50 µM for NAD(H) and 0.2 to 100 µM for all other compounds. The internal standard mix consisted of $^2H_3$-lactate (100 µM), $^2H_7$-glucose (133 µM), $^{13}C_3$-^{15}N-serine (100 µM) and $^2H_4$-NAD^+(25 µM). 20 µl internal standard mix was added to 400 µl methanol cell extract or 50 µl calibration standard. Samples were evaporated under a gentle nitrogen flow at 40 °C. Dry extracts were reconstituted in 50 µl 50/50 acetonitrile/Milli-Q water and transferred to LC vials.

Analysis was performed using an Ultimate 3000 UHPLC system (Thermo Fisher Scientific) coupled to a Q Exactive HF hybrid quadrupole-Orbitrap mass spectrometer (Thermo Fisher Scientific) equipped with a heated electrospray ionization (HESI) source. The equipment was routinely purged and recalibrated before each measurement sequence. 5 µl sample was injected on an Atlantis Premier BEH Z-HILIC column (1.7 µm, 2.1 x 100 mm; Waters) with a flow rate of 0.5 ml/min, column oven temperature of 40 °C and autosampler temperature of 10 °C. Solvent A was comprised of 20 mM ammonium bicarbonate (pH 9.00) in Milli-Q water and solvent B was comprised of 20 mM ammonium bicarbonate in acetonitrile. Gradient elution was as follows: 0 to 5 min linear gradient from 90-65% B, 5 to 6 min isocratic 65% B, 6 to 6.5 min linear gradient from 65 to 90% B, 6.5-12 to 5 min column equilibration at 90% B. The mass spectrometer was operated in positive and negative mode with the following scan parameters: capillary voltage of 4 kV, AGC target of 1 x 10^6, resolution of 120,000, maximum injection time of 200 ms, capillary temperature of 350 °C and an S-lens RF level of 75. Data acquisition was done using Xcalibur software. To identify and reduce potential contamination, blanks were measured between samples. Peak integration was done using Tracefinder software (Thermo Fisher Scientific; version 4.1). For representative chromatograms of endogenous metabolites and internal standards, see Fig. S5*C–D*.

Data analysis

Metabolite concentrations obtained by LC-MS were corrected for protein concentration using a Pierce BCA protein assay, which was performed according to the manufacturer's protocol (Thermo Fisher Scientific). Fractional labeling was calculated by dividing the isotopologue concentration or peak intensity by the summed concentration or intensity of all isotopologues.

For statistical analysis, GraphPad Prism (Version 10.1.2) was used. Parametric unpaired two-tailed student's t-tests were

used to compare technical triplicates of control and treated cells. If applicable, Benjamini-Hochberg correction was applied to correct for multiple comparisons. (Adjusted) p-value < 0.05 was considered statistically significant. Fold change was calculated by dividing individual concentration or intensity values by the geometric mean of control samples. Fractional turnover (K) of isotope-labeled metabolites was calculated by nonlinear regression of the fractional labeling over time (32).

Data availability

The authors confirm that the data generated in this study to support the findings is available within the manuscript and the supporting information.

Supporting information—This article contains supporting information.

Author contributions—J. J. M. J., N. M. V., J. C., and H. M. G. writing–review & editing; J. J. M. J. and N. M. V. supervision; J. J. M. J. and N. M. V. methodology; J. J. M. J., N. M. V., and H. M. G. conceptualization. H. M. G. writing–original draft; H. M. G. investigation; H. M. G. formal analysis.

Funding and additional information—This work was funded by a Catalyst Grant from United for Metabolic Diseases (UMD-CG-2022–007), which is financially supported by Metakids, awarded to H. M. G., J. J. M. J. and N. M. V.-D.

Conflicts of interest—The authors declare that they have no conflicts of interest with the contents of this article.

Abbreviations—The abbreviations used are: ACSM, acyl-coA synthetase medium chain; CI-IV, complex I-IV; DI-HRMS, direct infusion high-resolution mass spectrometry; G3P, glycerol-3-phosphate; GAPDH, glyceraldehyde 3-phosphate dehydrogenase; GDH, glutamate dehydrogenase; IMD, inborn metabolic disease; LC-FAOD, long-chain fatty acid oxidation disorder; MCAD, medium-chain acyl-CoA dehydrogenase; MCT, medium-chain triglyceride; MPC, mitochondrial pyruvate carrier; MTP, mitochondrial trifunctional protein; OAA, oxaloacetate; PC, pyruvate carboxylase; PDH, pyruvate dehydrogenase; PHGDH, phosphoglycerate dehydrogenase; SCAD, short-chain acyl-CoA dehydrogenase; TCA, tricarboxylic acid; VLCAD, very long chain acyl-coA dehydrogenase.

References

1. Hanson, R. W., and Patel, Y. M. (1994) Phosphoenolpyruvate carboxykinase (GTP): the gene and the enzyme. *Adv. Enzymol. Relat. Area Mol. Biol.* **69**, 203–281
2. Hellerstein, M. K. (1999) De novo lipogenesis in humans: metabolic and regulatory aspects. *Eur. J. Clin. Nutr.* **53**(Suppl 1), S53–S65
3. Hunter, G. A., and Ferreira, G. C. (2011) Molecular enzymology of 5-aminolevulinate synthase, the gatekeeper of heme biosynthesis. *Biochim. Biophys. Acta* **1814**, 1467–1473
4. Owen, O. E., Kalhan, S. C., and Hanson, R. W. (2002) The key role of anaplerosis and cataplerosis for citric acid cycle function. *J. Biol. Chem.* **277**, 30409–30412
5. Marin-Valencia, I., Roe, C. R., and Pascual, J. M. (2010) Pyruvate carboxylase deficiency: mechanisms, mimics and anaplerosis. *Mol. Genet. Metab.* **101**, 9–17
6. Roe, C. R., and Mochel, F. (2006) Anaplerotic diet therapy in inherited metabolic disease: therapeutic potential. *J. Inherit. Metab. Dis.* **29**, 332–340
7. Shirley, M. (2020) Triheptanoin: first approval. *Drugs* **80**, 1595–1600
8. Vockley, J., Marsden, D., McCracken, E., DeWard, S., Barone, A., Hsu, K., *et al.* (2015) Long-term major clinical outcomes in patients with long chain fatty acid oxidation disorders before and after transition to triheptanoin treatment–A retrospective chart review. *Mol. Genet. Metab.* **116**, 53–60
9. Vockley, J., Burton, B., Berry, G. T., Longo, N., Phillips, J., Sanchez-Valle, A., *et al.* (2017) UX007 for the treatment of long chain-fatty acid oxidation disorders: safety and efficacy in children and adults following 24weeks of treatment. *Mol. Genet. Metab.* **120**, 370–377
10. Gillingham, M. B., Heitner, S. B., Martin, J., Rose, S., Goldstein, A., El-Gharbawy, A. H., *et al.* (2017) Triheptanoin versus trioctanoin for long-chain fatty acid oxidation disorders: a double blinded, randomized controlled trial. *J. Inherit. Metab. Dis.* **40**, 831–843
11. Vockley, J., Burton, B., Berry, G. T., Longo, N., Phillips, J., Sanchez-Valle, A., *et al.* (2019) Results from a 78-week, single-arm, open-label phase 2 study to evaluate UX007 in pediatric and adult patients with severe long-chain fatty acid oxidation disorders (LC-FAOD). *J. Inherit. Metab. Dis.* **42**, 169–177
12. Schiffmann, R., Wallace, M. E., Rinaldi, D., Ledoux, I., Luton, M. P., Coleman, S., *et al.* (2018) A double-blind, placebo-controlled trial of triheptanoin in adult polyglucosan body disease and open-label, long-term outcome. *J. Inherit. Metab. Dis.* **41**, 877–883
13. Borges, K., Kaul, N., Germaine, J., Kwan, P., and O'Brien, T. J. (2019) Randomized trial of add-on triheptanoin vs medium chain triglycerides in adults with refractory epilepsy. *Epilepsia Open* **4**, 153–163
14. Laemmle, A., Steck, A. L., Schaller, A., Kurth, S., Perret Hoigné, E., Felser, A. D., *et al.* (2021) Triheptanoin - novel therapeutic approach for the ultra-rare disease mitochondrial malate dehydrogenase deficiency. *Mol. Genet. Metab. Rep.* **29**, 100814
15. Striano, P., Auvin, S., Collins, A., Horvath, R., Scheffer, I. E., Tzadok, M., *et al.* (2022) A randomized, double-blind trial of triheptanoin for drug-resistant epilepsy in glucose transporter 1 deficiency syndrome. *Epilepsia* **63**, 1748–1760
16. Karunanidhi, A., Van't Land, C., Rajasundaram, D., Grings, M., Vockley, J., and Mohsen, A. W. (2022) Medium branched chain fatty acids improve the profile of tricarboxylic acid cycle intermediates in mitochondrial fatty acid β-oxidation deficient cells: a comparative study. *J. Inherit. Metab. Dis.* **45**, 541–556
17. Ramsay, R. R., Gandour, R. D., and van der Leij, F. R. (2001) Molecular enzymology of carnitine transfer and transport. *Biochim. Biophys. Acta* **1546**, 21–43
18. Latipää, P. M., Peuhkurinen, K. J., Hiltunen, J. K., and Hassinen, I. E. (1985) Regulation of pyruvate dehydrogenase during infusion of fatty acids of varying chain lengths in the perfused rat heart. *J. Mol. Cell Cardiol* **17**, 1161–1171
19. Broeks, M. H., Meijer, N. W. F., Westland, D., Bosma, M., Gerrits, J., German, H. M., *et al.* (2023) The malate-aspartate shuttle is important for de novo serine biosynthesis. *Cell Rep.* **42**, 113043
20. Brunengraber, H., and Roe, C. R. (2006) Anaplerotic molecules: current and future. *J. Inherit. Metab. Dis.* **29**, 327–331
21. Kajimoto, M., Ledee, D. R., Olson, A. K., Isern, N. G., Des Rosiers, C., and Portman, M. A. (2015) Differential effects of octanoate and heptanoate on myocardial metabolism during extracorporeal membrane oxygenation in an infant swine model. *Am. J. Physiol. Heart Circ. Physiol.* **309**, H1157–H1165
22. Lund, M., Heaton, R., Hargreaves, I. P., Gregersen, N., and Olsen, R. K. J. (2023) Odd- and even-numbered medium-chained fatty acids protect against glutathione depletion in very long-chain acyl-CoA dehydrogenase deficiency. *Biochim. Biophys. Acta Mol. Cell Biol. Lipids* **1868**, 159248

23. Yang, E., Kruger, E., Yin, D., Mace, K., Tierney, M., Liao, N., *et al.* (2024) Major clinical events and healthcare resource use among patients with long-chain fatty acid oxidation disorders in the United States: results from LC-FAOD Odyssey program. *Mol. Genet. Metab.* **142**, 108350
24. Okere, I. C., McElfresh, T. A., Brunengraber, D. Z., Martini, W., Sterk, J. P., Huang, H., *et al.* (2006) Differential effects of heptanoate and hexanoate on myocardial citric acid cycle intermediates following ischemia-reperfusion. *J. Appl. Physiol. (1985)* **100**, 76–82
25. Watford, M., Erbelding, E. J., and Smith, E. M. (1987) The regulation of glutamine and ketone-body metabolism in the small intestine of the long-term (40-day) streptozotocin-diabetic rat. *Biochem. J.* **242**, 61–68
26. Tucci, S., Behringer, S., and Spiekerkoetter, U. (2015) De novo fatty acid biosynthesis and elongation in very long-chain acyl-CoA dehydrogenase-deficient mice supplemented with odd or even medium-chain fatty acids. *FEBS J.* **282**, 4242–4253
27. Tucci, S., Primassin, S., Ter Veld, F., and Spiekerkoetter, U. (2010) Medium-chain triglycerides impair lipid metabolism and induce hepatic steatosis in very long-chain acyl-CoA dehydrogenase (VLCAD)-deficient mice. *Mol. Genet. Metab.* **101**, 40–47
28. Tucci, S. (2017) Very long-chain acyl-CoA dehydrogenase (VLCAD-) deficiency-studies on treatment effects and long-term outcomes in mouse models. *J. Inherit. Metab. Dis.* **40**, 317–323
29. Haijes, H. A., Willemsen, M., Van der Ham, M., Gerrits, J., Pras-Raves, M. L., Prinsen, H., *et al.* (2019) Direct infusion based identifies metabolic disease in patients' dried blood spots and plasma. *Metabolites* **9**, 12
30. Meijer, N. W., Zwakenberg, S., Gerrits, J., Westland, D., Ardisasmita, A. I., Fuchs, S. A., *et al.* (2024) Direct infusion mass spectrometry to rapidly map metabolic flux of substrates labeled with stable isotopes. *Metabolites* **14**, 246
31. Meijer, N. W. F., Gerrits, J., Zwakenberg, S., Zwartkruis, F. J. T., Verhoeven-Duif, N. M., and Jans, J. J. M. (2023) Metabolic alterations in NADSYN1-deficient cells. *Metabolites* **13**, 1196
32. Patterson, B. W. (1997) Use of stable isotopically labeled tracers for studies of metabolic kinetics: an overview. *Metabolism* **46**, 322–329